Computer Simulation of Electron-Beam Resist Profiles

A user-oriented, conversational computer program, LMS (Lithography Modeling System), has been developed for rapid investigation of the total lithographic process used in electron-beam lithography, including electron exposure and resist development. Electron scattering and energy deposition within the resist film are simulated with Monte Carlo techniques, including the significant effects of electrons backscattered from the substrate. The magnitude of and correction for the resulting intra- and inter-line proximity effects in the latent image and their dependence on variables such as beam voltage, film thickness, substrate material, and line-pattern geometries are easily investigated with LMS. The latent image in the resist film is transformed into a solubility-rate image. The time evolution of the developed-resist profile and its dependence on electron dose, solvent, etc. can also be determined.

Introduction

The technology of electron-beam (e-beam) lithography depends on the complex interaction of a focused e-beam with a polymer film on a nonpolymeric substrate. Electron irradiation of a polymer film produces chemical changes such as polymer chain scission (positive resist) or polymer chain cross-linking (negative resist), giving rise to areas with different solubility properties. Selective organic solvents are then used to develop the film in patterns that correspond to the electron irradiation pattern. The remaining polymer film can be used subsequently as a resist mask for substrate etchants or metal film deposition. Electron beams, along with x-ray and deep uv optical methods, are now being used to replace conventional uv contact printing for the fabrication of semiconductor and magnetic bubble integrated circuits [1].

The spatial contours or profiles developed in the polymer film are determined by two separate processes: 1) electron scattering and energy deposition within the film and 2) chemical development of the electron-irradiated volume with a solvent. Due to the large number of experimental variables encountered in these processes, it is very desirable to have a simulation tool to study the importance and consequence of the various process parameters in the context of the entire lithography process. For a

particular application, it is also important to optimize parameters such as e-beam voltage, resist film thickness, electron dose, developer type and time, etc., to achieve a desired resist profile. In particular, it is very important to quantitatively understand and compensate for the so-called *proximity effects* unique to e-beam lithography. These effects are due to electron scattering within the film-substrate target and appear in isolated lines (intraline proximity effects) and line arrays (inter-line proximity effects). Hence, the actual dose absorbed by a pattern feature depends on both its size and neighboring features [2, 3]. As feature sizes and spacings become smaller, proximity effects become larger; hence, they impact the maximum device density in very large scale integration (VLSI) technology.

In this paper we describe a software package called LMS (Lithography Modeling System), which simulates the two processes of electron scattering and subsequent development to predict the time-evolution of line profiles developed in an e-beam resist film. The model automatically includes proximity effects and can also be used to calculate the dose modulation or feature-size modulation necessary to compensate for proximity effects, including the developer process. A description is given of the soft-

Copyright 1980 by International Business Machines Corporation. Copying is permitted without payment of royalty provided that (1) each reproduction is done without alteration and (2) the *Journal* reference and IBM copyright notice are included on the first page. The title and abstract may be used without further permission in computer-based and other information-service systems. Permission to *republish* other excerpts should be obtained from the Editor.

ware system and its use in a conversational mode on a graphics computer terminal. Some relevant and exploratory examples of LMS applications are also given.

Electron scattering and energy deposition in resist films

Monte Carlo simulation of electron scattering is used, coupled with a model for energy loss along the electron trajectory, to calculate the spatial distribution of energy deposited in the resist film by an e-beam. This spatial distribution is referred to as the *latent image*. The details of the Monte Carlo simulation have been given previously [4], but a brief outline is presented here. Figure 1 shows a sequence of scattering events for one electron with energy E_0 incident on a resist film with thickness t.

The step length Λ is the energy-dependent mean free path for elastic scattering of the electron by an atom. The scattering angles θ_n and ϕ_n are chosen with the aid of computer-generated random numbers. Energy loss along the step length is given by a continuously-slowing-down approximation. The resist film volume is divided into small cells and the energy deposited within each cell is accumulated from any and all electrons that traverse it. For statistical precision, a large number $(1-2 \times 10^4)$ of electron trajectories are simulated to form the latent image, since no two electrons will have the same trajectory. Some electrons enter the substrate and can be scattered back into the film at large lateral distances from their point of entry. This produces a broad tail in the radial distribution of the latent image. This radial distribution originates in the Monte Carlo simulation as a histogram with spatial resolution equal to the particular cell size. The latent image is actually the group of radial distributions at each successive depth in the film. For a 1- μ m film with a cell size of 0.05 μ m there are 20 such distributions and each distribution is different due to the degree of electron scattering at each depth z. The distribution also depends on the geometry of the source (e.g., point or line source). For a line source, the radial distribution is integrated along the line axis.

Radial distributions can be curve-fitted by approximation with two coaxial Gaussian distributions [5], but in simulation of the developed profile we prefer to retain the accuracy in the basic Monte Carlo histogram and carry it through all subsequent calculations. The Monte Carlo simulation can automatically accommodate the discontinuity between the film and substrate since the electron position is known and the scattering parameters associated with each particular material are changed as the electron crosses the boundary. Non-Monte Carlo techniques must, out of necessity, treat any electrons backward-scattered from the substrate with a different model from that

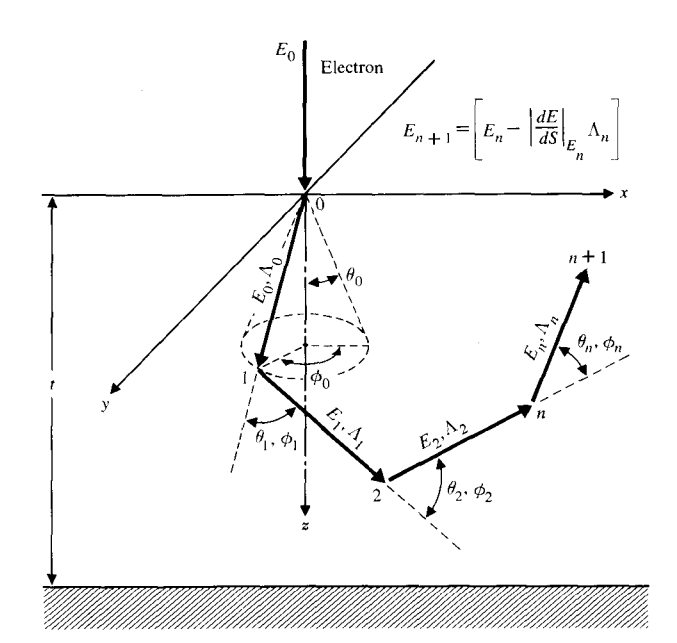


Figure 1 Schematic diagram showing the initial Monte Carlo step lengths for electron scattering in a thin resist film on a thick substrate.

used for forward-scattered electrons. The artificial separation of forward- and backward-scattered electrons may lead to some uncertainties in the present application. As we will see, the contribution of the backward-scattered electrons to the latent image is an important factor in proximity effects. The remainder of this paper discusses only y-directed line sources of electron exposure, and the simulated profiles are in cross-section to the line axis.

The present version of the Monte Carlo program requires about 1 min of CPU time per 10³ trajectories, and a latent image needs to be calculated only once for a particular target configuration and beam voltage. Any arbitrary film and substrate material can be modeled. In addition, we can account for a second film between the resist and substrate, such as is encountered in optical mask making.

Initially, the spatial distribution of energy absorbed in the resist film by a δ -function line source is calculated. With the δ -function latent image in the form of a two-dimensional histogram of energy density (eV/cm³) in x and z (with resolution $\delta x = \delta z$), the spatial distribution of energy density in the resist film can be calculated for any arbitrary incident beam shape. For a round beam source such as that produced in a vector-scan system [6], the incident beam profile can be described by a Gaussian distribution. For a square beam source such as that produced in the IBM-EL1 system [7], the beam profile can be described by a convolution of a Gaussian distribution

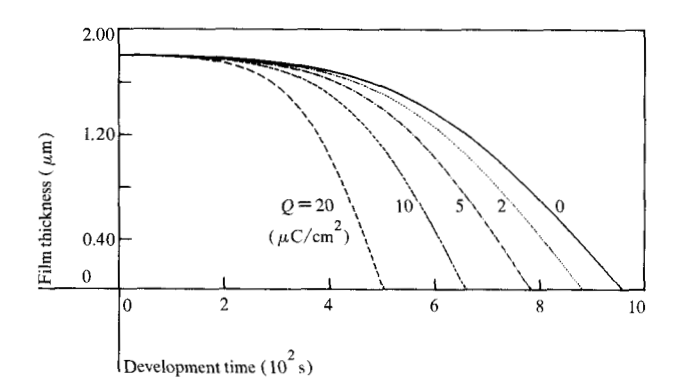


Figure 2 Thickness of resist remaining vs, development time for an etching rate given by Eq. (3); rate parameters as in the text.

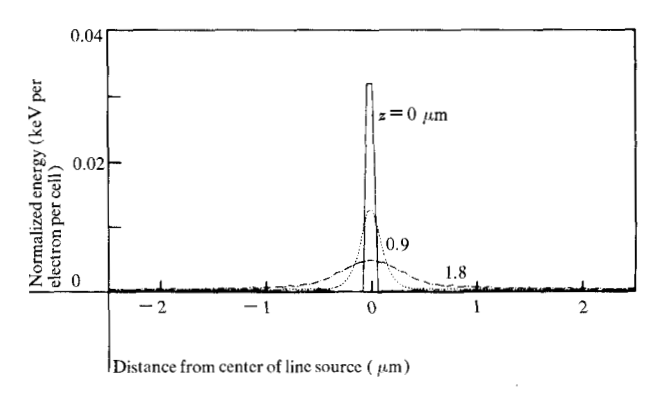


Figure 3 Lateral distribution of energy deposited in the film of 1.8- μ m polymeric resist on Si (25 keV, 2.0- μ m written linewidth) using a Monte Carlo simulation for an ideal line source.

with itself over the square dimension. The result of such a convolution is given [3] as a sum of error functions (erf):

$$f(x) = K\{\operatorname{erf}\left[(a-x)/\sigma\sqrt{2}\right] + \operatorname{erf}\left[(a+x)/\sigma\sqrt{2}\right]\}, \quad (1)$$

where the beamwidth (FWHM) = 2a, σ is the standard deviation, and K is a constant. For $a/\sigma >> 1$, the edge slope is

$$\left| \frac{df}{dx} \right|_{x=\pm a} = \frac{2K}{\sigma \sqrt{2\pi}} \,. \tag{2}$$

The edgewidth EW is given by $\sigma\sqrt{2\pi}/2$, and is defined by the tangent line to $f(\pm a)$ intercepting f(x) = 0 and f(x) = 2K erf $(a/\sigma\sqrt{2})$. The edge of f(x) is symmetric about its half height.

Since LMS was originally designed to simulate the lithography process associated with the IBM-EL1 tool, we use Eq. (1) as an envelope function for digital convolution of the latent image from an ideal line source. This convolution results in significant savings in computer time compared to distributing the electrons over a finite beamwidth within the Monte Carlo simulation [3]. The convolution assumes that superposition of electron exposure and subsequent energy deposition holds.

Developer characterization

To simulate the time-evolution of the developed profile, we must transform the latent image into a solubility-rate image. For such a transformation, we need to establish a relationship between local solubility rate R (nm/s) and local absorbed energy density E (eV/cm³). By using Erather than incident electron flux Q (C/cm²) we remove any artificial dependence of solubility rate on beam voltage. Since at present this relationship between R and E cannot be established from theory, we must depend on experimental measurements of changes in film thickness vs. development time for a particular film-solvent combination and dose Q. After curve-fitting such data with an analytical expression including the Q-dependence of R, we can then use the expression with LMS. However, most measurements in one dimension only specify R(z)vs. Q. Thus, the Monte Carlo simulation must also be used to transform Q into E(z) for a plane source; see for example Figs. 2(a)-(b) in Ref. [4]. The latent image for a finite feature will be a function of cell position (i.e., x and z); hence, the solubility rate image will also be a function of x and z. The solubility rate image is subsequently transformed into a profile evolution via a cell model for dissolution similar to that described in simulation of optical lithography [8]. Both positive and negative resists can be simulated within LMS.

After some experience with a variety of resist materials and solvents, we found that the following general relationship between R and E adequately describes the observed one-dimensional rate data for positive resists:

$$R = (A + BE^n)(1 - e^{-\alpha z}) + \varepsilon(E), \tag{3}$$

where R is the etch rate (nm/s), z is the distance below the film surface (μ m), E is the absorbed energy density (keV/cm³), and A, B, α , and n are appropriate constants. Note that $E \propto Q$. The dependence of ε is given by

$$\varepsilon(E) = \varepsilon_0 + CE^m, \tag{4}$$

where C and m are constants and E is evaluated at z=0. The form of Eq. (3) results in a special characteristic such that for $z << 1/\alpha$ and Q=0, $R=\varepsilon_0$. For $z>1/\alpha$ and Q=0, $R=A+\varepsilon_0$. This type of dissolution behavior for unexposed resist has been observed by several authors for diazo-type positive photoresist materials under both optical and e-beam exposures [9-10]. A hypothetical example of the thickness-time curves for such materials is shown in Fig. 2 with A=5 nm/s, $\alpha=1.5$ μ m⁻¹, $B=2.5\times10^{-18}$, n=1.05, $C=2.0\times10^{-30}$, m=1.5, and $\varepsilon_0=0.05$ nm/s. If

we let α become large and make C=0, Eq. (3) reduces to a form utilized previously to describe the solubility behavior of polymethylmethacrylate (PMMA) [11-13]. The new parameter α is interpreted to describe the distance that the solvent must diffuse into the resist before the onset of any significant solubility rate. This diffusion distance is then approximately $1/\alpha$. The term $\varepsilon(E)$ is a correction term to provide the proper surface rate.

Hence, Eq. (3) can be used to describe the solubility behavior of both "nonlinear" (e.g., *AZ-1350J [14]) and "linear" (e.g., PMMA) resists. This linearity or nonlinearity refers, of course, only to the unexposed resist and its solubility rate with depth. All resists are nonlinear when exposed by e-beams (i.e., R changes with depth z) due to electron scattering.

Details of the LMS programs, the system description, a flow chart, and the algorithms are contained in the Appendix. Also presented there is a portion of the actual computer terminal I/O text during an LMS session.

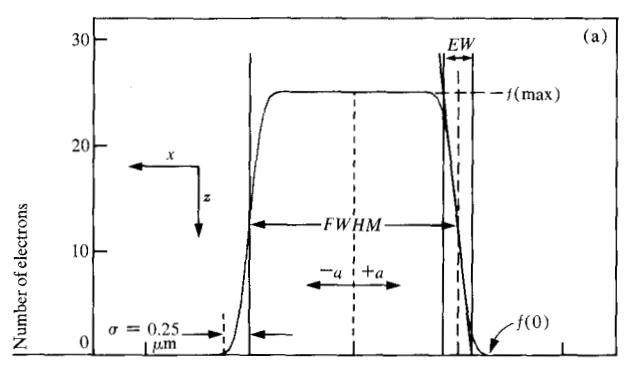
Example applications

We will now describe and illustrate the sequence of events for a simple example calculation with LMS, namely a $2-\mu m$ line written and developed in a $1.8-\mu m$ -thick resist with hypothetical development characteristics.

After execution of the MONTY EXEC routine (see Appendix), a two-dimensional histogram of energy deposited within each cell vs. cell position (x, z) is stored for a y-directed ideal line source. Figure 3 shows the simulated lateral profile of energy deposited within the resist film at three different levels for a 25-kV beam, 1.8- μ m film on Si. Near the surface $(z=0~\mu\text{m})$, the distribution is very narrow and intense. As the depth z increases, the distribution becomes broader and weaker and a significant "tail" appears because of electron backscattering from the substrate. Scattering of electrons both forward and backward contributes to the proximity effect in e-beam lithography.

After execution of the BEAMSHPE EXEC, a primary incident beam profile is formed [Fig. 4(a)]. This is the envelope curve under which the δ -function distribution (Fig. 3) will be convoluted.

After execution of the CONVOLUT EXEC, the twodimensional histogram of normalized energy density (eV/ C-cm) vs. cell position (x, z) is stored. The curves in Fig. 4(b) show the results of convolution for three different depths z in the film. Here, the energy deposited varies with z and the "tails" of the distribution in Fig. 3 are now a significant part of the total distribution.



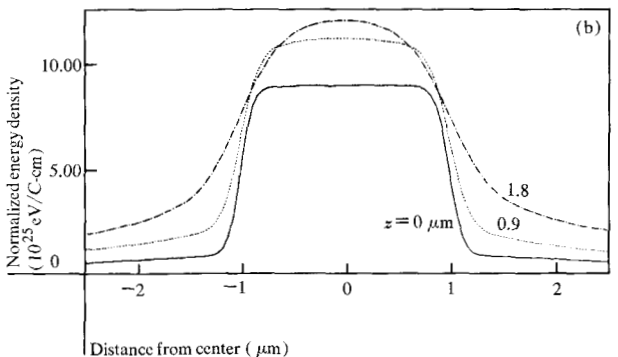


Figure 4 (a) Definition of terms. The vertical axis is the number of electrons distibuted over the incident line, normalized to 10^5 total electrons. Example profile describing the incident current density for a 2.0- μ m linewidth via Eq. (1). (b) The curves give the lateral distribution of energy deposited within a 1.8- μ m polymeric resist film (Si substrate) by 25-keV electrons for the 2.0- μ m written linewidth; $1 \text{ keV} = 1.602 \times 10^{-16} \text{ J}$. Throughout the text energy values are given in keV.

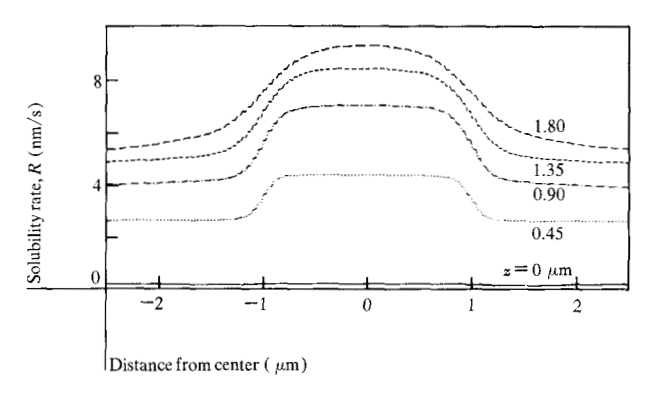


Figure 5 Lateral distribution of etch rate for the same resist film and the latent image of Fig. 4(b); $Q = 20 \mu \text{C/cm}^2$.

The latent image of Fig. 4(b) is transformed into a solubility rate image with Eq. (3) (DEVELOPE EXEC); see Fig. 5 for the special case of the rate values given previously and $Q = 20 \,\mu\text{C/cm}^2$. The developer algorithm also calculates the time-evolution of surface profiles by connecting together all the cells that have the same total development time. The development time for a particular

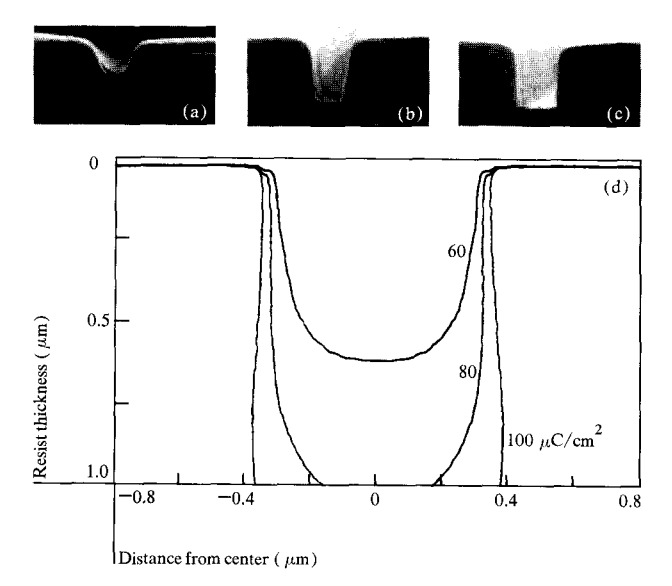


Figure 6 Cross-sectional SEMs of developed profiles in $1-\mu$ m PMMA resist for doses of (a) 60, (b) 80, and (c) 100μ C/cm² for an 0.5- μ m linewidth and 20-keV electrons. The profiles were developed in 1:1 MIBK-IPA for 3 min. (d) The simulated profiles.

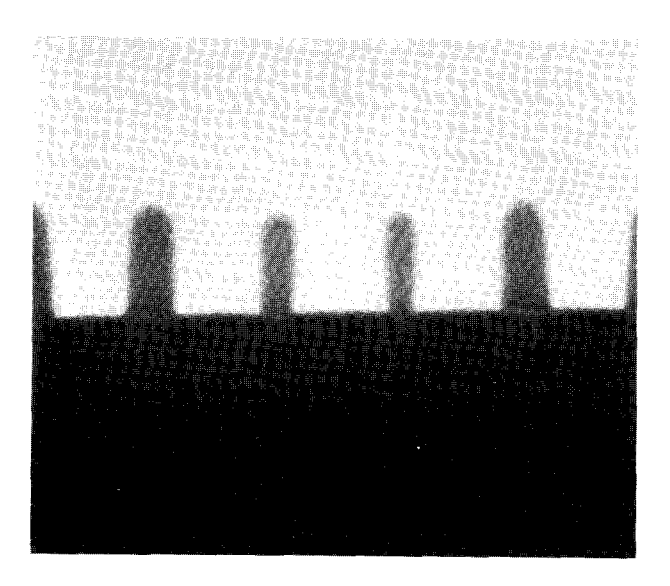


Figure 7 Cross-sectional SEM of developed profile in 1- μ m PMMA for a five-line array of 0.5- μ m lines and gaps.

cell, once it becomes exposed to the solvent, depends on the number of cell faces exposed, and therefore on the development time for its nearest and next-nearest neighbors. An example of the time-evolution for development of Fig. 5 is shown in the Appendix for TIME = 5, 7.5, and 10 min (see Fig. A5). The developer algorithm has several options that allow the user to specify such development conditions as the time of development in the profile simu-

lation; the depth of development, *i.e.* the profile which just reaches that depth; the open dimension (width of development) of the profile at a particular depth; or a particular point on a desired profile. Since input options are specified by the user during execution of the developer algorithm and a series of mixed options can be run sequentially, the profile simulation output is very flexible. In addition, the resist film can be divided into several layers and each layer can be developed with selective (or common) solvents, each with its appropriate developer characteristics.

• Isolated lines—theory and experiment

To assess the simulation accuracy, a test pattern consisting of isolated lines and five-line arrays with various linewidths was written in a 1-\mum-thick PMMA-type resist on Si substrates in our VS-1 lithography system [6] and exposed with different electron doses Q at a beam voltage of 20 keV. The resist was developed in a 1:1 solution of methylisobutylketone (MIBK) and isopropanol (IPA) for 3 min at room temperature. After we fractured the silicon perpendicular to the written line, the developed patterns were examined by scanning electron microscopy (SEM). Figures 6(a)-(c) show typical SEM micrographs of the isolated 0.5-\(\mu\)m lines for incident electron doses of 60, 80, and $100 \,\mu\text{C/cm}^2$, respectively. From such observations, one can ascertain the relative "sensitivity" of various resist materials by using criteria such as the dose required to obtain perpendicular sidewalls [15].

For the simulation, the magnitude of the rate parameters in Eq. (3) were determined for the same PMMA resist developer by exposing large pads in the resist at various doses and measuring the thickness loss vs. development time. After converting Q to E as described earlier, the solubility rate R (nm/s) was plotted vs. E. The appropriate rate constants were then determined by curve fitting [13]. For the resist used in this experiment, the rate constants are A = 0.1 nm/s, $a = \infty$, $B = 6.4 \times 10^{-37} (\text{cm}^3/\text{keV})^2$, n =2.0, and $\varepsilon_0 = C = 0$. The value of B can be determined by an intersection point D_0 between the tangents to the lowand high-dose portions of the rate curve on a log-log plot; it is a fixed quantitative number, as are A and n. For $D_0 =$ $200 \text{ J/cm}^3 = 1.25 \times 10^{18} \text{ keV/cm}^3$ (the value used previously [13]), we can also evaluate B for use in Eq. (3) since $B = (1/D_0)^n$.

The only other parameter to be determined for LMS is the value of σ in Eq. (1). Since this is not directly measurable in our VS-1 system, we have deduced an effective σ by searching for the best agreement between the observed and simulated profiles. After comparison with a variety of developed profiles, we have arrived at the following effective values: $\sigma = 0.12~\mu m$ and $B = 8.0 \times 10^{-37}$

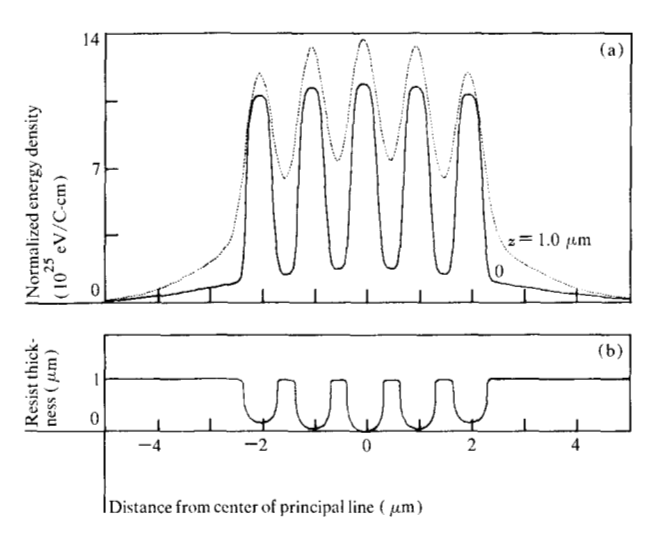


Figure 8 (a) The curves give the lateral distribution of energy deposited in the film by 20-keV electrons at different levels in the film. The incident exposure is a five-line array as in Fig. 7. (b) The simulated profile for the latent image using developer parameters: A = 0.1 nm/s, $B = 8.0 \times 10^{-37} \text{ (cm}^3\text{/keV})^2$, and n = 2.0 (appropriate for PMMA in 1:1 MIBK-IPA). Only the profile corresponding to the first line to reach the substrate (Si) surface is shown; $Q = 80 \mu\text{C/cm}^2$.

 $(cm^3/keV)^2$. This value for σ is reasonable, and the effective value for B is very close to that obtained from the one-dimensional rate-curve fitting. The small difference may be due to the use of an average value for E within the film for conversion of Q to E, rather than considering the z-dependence of E. There may also be a small systematic experimental error and, of course, we have assumed the incident beam in our VS-1 system to be Gaussian in profile.

The curves in Fig. 6(d) show the result of using LMS to simulate the 3-min developed profile in the same PMMA resist for the same electron doses of 60, 80, and 100 μ C/cm², respectively, and using the same rate constants discussed previously. Direct comparison with Figs. 6(a)-(c) shows good agreement in shape and dose dependence. The top corner edges of the simulated profiles are noticeably sharper than the observed corners. Similar agreement and differences were observed for a variety of isolated lines and linewidths. With the variety of parameters contained within the total simulation, including those associated with electron scattering and solvent development, this relatively good agreement between theory and experiment is very encouraging.

• Inter-line proximity effect in line arrays

Because of electron scattering, the various lines in a finite line array do not develop to the same size at the same time. For example, Fig. 7 shows a five-line array of 0.5- μ m lines and 0.5- μ m gaps written in 1 μ m of a PMMA-

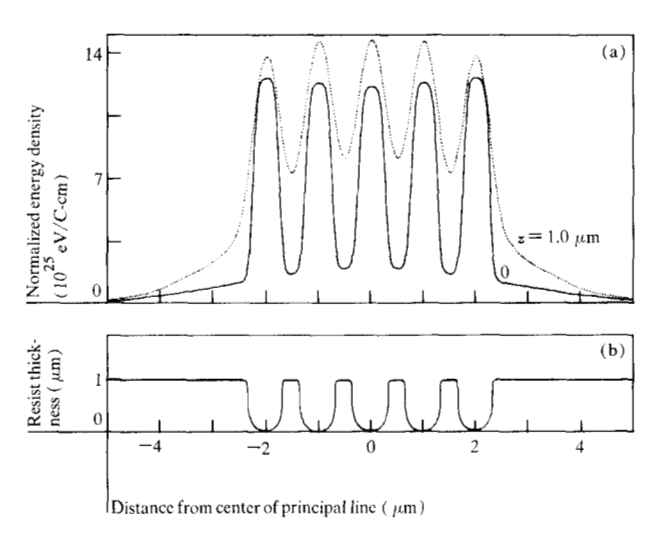
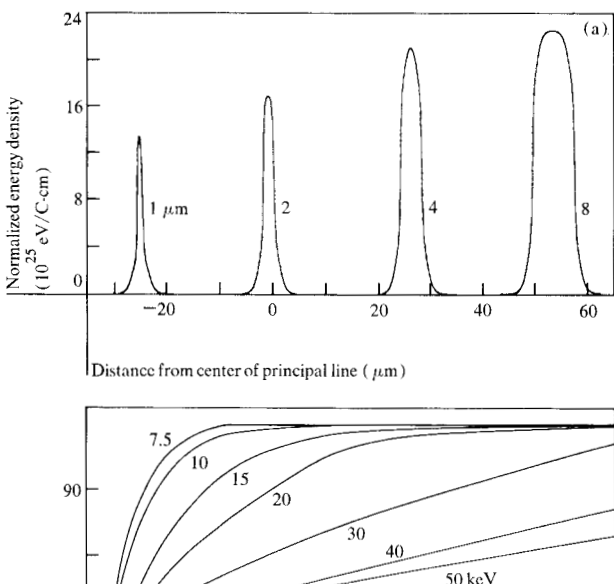


Figure 9 (a) The curves give the lateral distribution of energy deposited at different levels in the resist film of Fig. 7 with dose modulation of 1.111 on the outer two lines and 1.041 on the inner two lines (1.000 for the center line) of the five-line array of 0.5- μ m lines and gaps. (b) Simulated developed profile for the latent image in (a). Note that all five lines now reach the substrate surface at the same time; $Q = 80 \ \mu \text{C/cm}^2$, developer parameters as in Fig. 8(b).

type resist. The two outer lines are narrower than the three inner ones. We can use LMS to study such interline proximity effects. A simulation of the absorbed energy density $(eV/cm^3)\ vs$. lateral distance is given in Fig. 8(a) for two depths in the film. Although each line received the same incident dose Q (C/cm²) on the surface, each did not receive the same absorbed energy density E (eV/cm³) within the film. Shown in Fig. 8(b) is the simulation of such a developed profile for a case where the central line just begins to open at the interface (represented by the horizontal line). The time evolution of the profile results in a nonuniform linewidth array, as was observed in Fig. 7.

With proper dose modulation of each line exposure about some nominal dose, the lines can be developed to the same size at the same time and LMS can be used to predict the proper dose modulation required for a particular line pattern and resist-developer system. With the DOSECORR EXEC, the user simply specifies the depth z at which the peak absorbed energy density is to be made uniform. The program then automatically iterates the relative line doses and converges to a unique dose modulation for each line to achieve this. For the five-line array of 0.5- μ m lines and gaps, the dose modulation required at depth $z = 0.5 \,\mu\text{m}$ is calculated to be 1.111 for the outer two lines and 1.041 for the inner two lines, with respect to a value of 1.000 for the central line. The corresponding latent images with this dose modulation are shown in Fig. 9(a); the developed image, in Fig. 9(b). The dose modula-



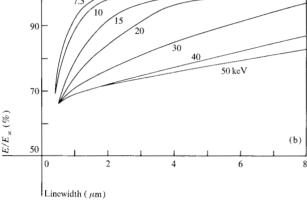


Figure 10 (a) Lateral distribution of energy deposited in the 1- μ m PMMA resist film of Fig. 7 for isolated lines with different linewidths, which have received the same incident electron dose. (b) Energy absorbed at $z=0.5\,\mu$ m for a 0.5- μ m PMMA film, relative to a large linewidth at the same beam voltage. The incident electron dose is the same for varying linewidth and constant beam voltage.

tion required will depend on film thickness, beam voltage, and line-pattern geometry. For calculating the proximity corrections to complex patterns of finite features, an analytical method has been developed that utilizes two coaxial Gaussian distributions to approximate the latent image in the resist film [16]. A variety of operating conditions have been calculated with Monte Carlo simulation of electron scattering, and a table of Gaussian parameters have been generated for use in such algorithms [5]. However, with LMS the developer effects can be included in the calculation of proximity effects and the actual resist profile is simulated in cross-section for evaluation and optimization.

• Intra-line proximity effects and their voltage dependence

Intra-line proximity effects due to electron scattering exist even for isolated lines and result in a linewidth depen-

dence of the absorbed energy density E. That is, per unit dose Q, narrow lines receive less internal energy deposition than do wider lines. As an example, Fig. 10(a) shows a series of latent image distributions of energy density for various linewidths in 1 μ m of PMMA at 20 keV. The distribution shown applies only to the depth z=1 μ m. At sufficiently large linewidths, the maximum value of E within the line reaches an asymptotic value corresponding to that for a large-pad exposure. The linewidth for which this occurs is determined by the maximum electron range and hence by the incident beam voltage. This distribution can go beyond ± 5 μ m (around center) at 25 keV. Thus, the beam voltage is an important factor in determining the magnitude of both inter- and intra-line proximity effects and their compensation via dose modulation.

Figure 10(b) shows the result of LMS simulation with varying linewidths and beam voltages for a 0.5- μ m resist. The value of the peak energy density within each isolated line has been normalized to that for a very large linewidth. For a particular beam voltage and linewidth, where this relative energy density approaches 100%, all lines with larger linewidths will have received the same energy density and will develop to the proper size simultaneously. For 10 keV, this minimum linewidth is $\approx 2 \mu m$; for 20 keV, it is $\approx 5 \mu m$. In practice, it may be sufficient to consider the relative energy to be $\geq 90\%$, in which case the minimum linewidths for 10 and 20 keV become about 1 and 3 μm , respectively. Similar curves are found for 1- μm -thick resist, but are shifted to larger linewidths.

Since any practical correction for proximity effects will be only approximate, it is advantageous to minimize the proximity effects by optimizing the e-beam/resist film interaction. For 0.5-\mu m resist films, such as those used in optical mask making, it is better to use 10 rather than 25 keV to achieve 1-μm minimum feature sizes; below about 1-µm linewidth at 10 keV, significant proximity effects appear, which must be corrected for in 0.5- μ m films. It is also apparent from Fig. 10(b) that for a range of small feature sizes, it is advantageous to use very high beam voltages (e.g., 50 keV) to provide uniform absorbed energy density. When the energy density is uniform, the various feature sizes are expected to develop to the proper size simultaneously, assuming the absence of any developer effects within the proximity effect. If the energy density cannot be made uniform from feature to feature by optimizing the beam voltage, a correction must be made during exposure via a complex pattern processor for proximity compensation. In the simplest case, one should be able to avoid the need for correction of proximity effects by using thin resist films and low beam voltages for features $>1\mu m$.

These predictions of the voltage dependence of proximity effects were tested by writing narrow lines in a five-line array pattern in 0.5- μ m resist at 10 and 20 keV. Figures 11(a) and (b) show optical micrographs of the 1- μ m (left) and 2- μ m (right) line arrays after development to size. At 20 keV, the outer two lines in the 1- μ m array are narrower than the inner three and in the 2- μ m case there is still some thickness loss between the lines. At 10 keV, the 1- μ m lines are uniform in size and there is no thickness loss between the 2- μ m lines. Hence, the experimental results support the LMS predictions.

• Multilayer resist films

One of the techniques used to obtain an undercut (lift-off) profile with relatively low electron dose involves use of a two-layered resist coating with selective solvents for each layer. The top layer is a high-sensitivity resist while the bottom layer is a lower-sensitivity or even radiation-insensitive material. After the image is formed in the top layer, it acts as a mask for subsequent development. Such a process has recently been used to fabricate 1-µm MOSFET VLSI devices [17]. When used to simulate such a condition, LMS can be useful in optimizing the configuration with respect to layer thicknesses, electron dose required, etc. As an example, Fig. 12 shows the simulated profile for a 0.5-\mu m nonlinear resist on a 1.3-\mu m linear resist for a 2.5-\mu m isolated linewidth written with an 80- μ C/cm² dose at 25 keV. The rate parameters used for the resist layers are the same hypothetical values as those used to generate Fig. 8 and the Appendix figure A5. It appears that a successful lift-off profile can be achieved. In these multilayered resist systems LMS can be used to rapidly investigate the tradeoffs among the large variety of experimental variables.

• Proximity function parameters

Some recent work [18] has shown that LMS can also be used to deduce the numerical values for the parameters in a proximity correction algorithm such as SPECTRE [16]. The dose compensation factors (DCF) for a variety of feature sizes were calculated with LMS including the developer effects. Then the SPECTRE program was iterated, for the same patterning, with a variety of input parameters for the coaxial Gaussian approximations $(\beta_f, \eta_E, \beta_h)$ until the DCF set agreed with the set derived from LMS. A unique set of parameters was found which provided the best agreement. For 1-\mu PMMA resist film on silicon at 20 keV, the best set is $\beta_f = 0.075 \mu m$, $\eta_E = 0.90$, $\beta_b =$ $2.75 \mu m$, and this set supports the conclusions reached by Parikh [19]. Hence it has now been demonstrated that resist profile simulation can be used successfully to predict reasonable values of the parameters in a proximity function without the necessity for an experimental matrix. This method of utilizing LMS will be particularly valuable

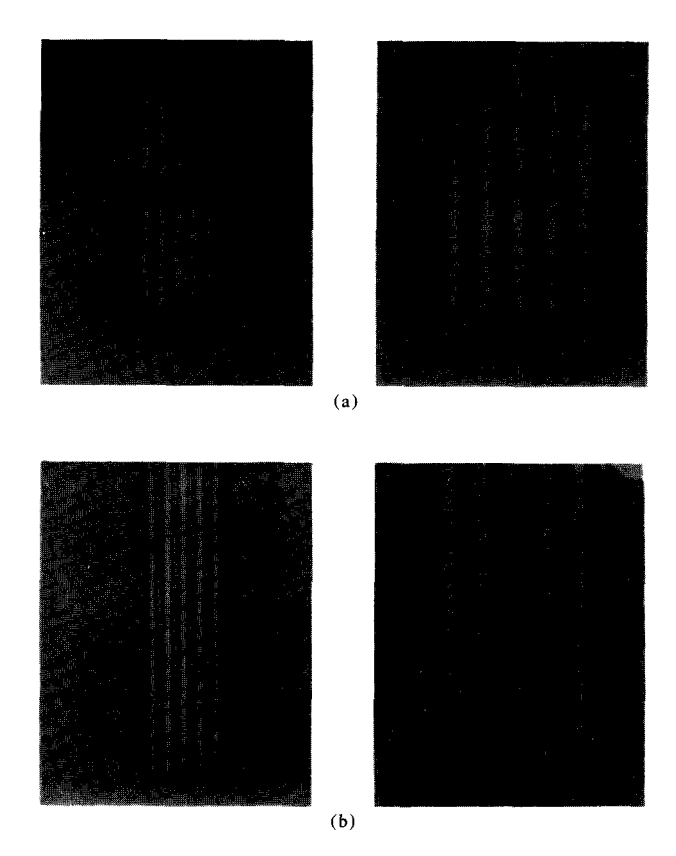


Figure 11 Optical micrographs of developed lines in a 0.5- μ m PMMA resist film for electron doses of (a) 40 μ C/cm², 10 keV and (b) 80 μ C/cm², 20 keV. The patterns are for five-line arrays of 1- μ m (left) or 2- μ m (right) lines and gaps.

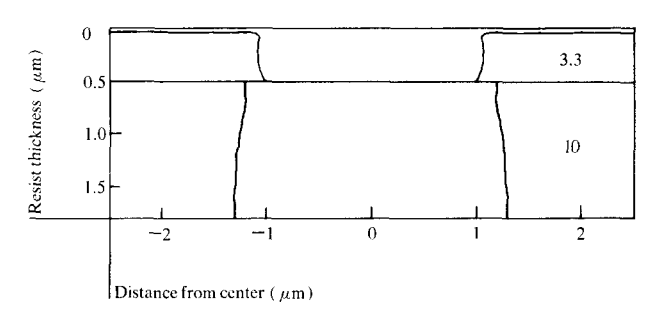


Figure 12 Simulated developed profile of a multilayer resist structure with total thickness of 1.8 μ m (0.5- μ m top layer, 1.3- μ m bottom layer). The development times are indicated for each layer.

for resist materials such as those shown in Fig. 2, which have unusual developer characteristics.

Summary

The application of new software for simulation of electron scattering, energy deposition, and subsequent development of the irradiated volume in a thin resist film has been described. This lithography modeling system (LMS) is very flexible and conversational with respect to the user. No detailed knowledge of the physics and chemistry used within the model is necessary. The LMS software is designed to be compatible with any VM/CMS system and is easily transported via computer network lines.

The one-dimensional development rate vs. electron exposure is the only experimental information required for simulation of developed resist profiles. When this information is input to LMS, the time evolution of the two-dimensional profiles for line exposure is simulated and the dominant physical parameters within the lithography process can be identified. Both inter- and intra-line proximity effects are automatically included within LMS, and the dependence of profile shape on beam voltage, electron dose, film thickness, substrate, and beam shape can be studied rapidly without resorting to a tedious matrix of experiments. In addition, the proximity function parameters for a proximity correction algorithm can be deduced, including the developer effects.

The quantitative accuracy of LMS has been verified by comparison with typical experimental profiles in PMMA films. The voltage dependence of the intra-line proximity effect has been studied theoretically via LMS and also experimentally. Both results show that for thin resist films such as those used in optical mask making, the intraline proximity effect needs no compensation (for low beam voltages) down to $\approx 1-\mu m$ linewidths. The benefits obtained with multilayer resist films for lift-off applications can also be explored with LMS. Work is presently in progress to incorporate within LMS subsequent lithography processes such as ion milling and plasma etching of the developed profile in the resist/substrate target, as well as three-dimensional images. This will provide the lithographer with a complete tool for optimizing a particular device process.

Appendix: LMS programs and system description

• Operating environment

The software package used to obtain the results presented in this paper operates in the VM/CMS environment. The basic sequential access method (BSAM) is used for disk file manipulation with variable spanned record source to accommodate free-format input/output (I/O). The real main storage requirements depend on the particular segment of the LMS package being executed.

• Source algorithms

The majority of the source algorithms in LMS are written in FORTRAN. A small minority are written in 360/370 assembler language. The choice of FORTRAN was based

primarily on portability and execution speed. Two features of FORTRAN that are used extensively are 1) unformatted disk and terminal I/O and 2) dimensionality in the MAIN routines only, with address passing and dynamic dimensions in the subroutines. All FORTRAN source code was compiled with the FORTHX compiler at an optimization level of 2.

• Basic LMS programming concepts and features

LMS was designed to be a VM/CMS EXEC-driven system. Each LMS function has a unique EXEC routine and a main source routine, the names of which are generally identical. The CMS-EXEC feature is used to provide user-defined implementation of sequential LMS functions.

The CMS "STACK" capability is used extensively to provide stacked terminal input data for passing parameters between EXEC and source routines. System support modules are used to examine file control block information of existing disk files. This information is used to determine the dimensionality requirements of arrays processed within the source code.

Graphic output is used extensively to display the vast amount of data generated by LMS; however, lists of the digital data are available. Graphics "windowing" and "scaling" provide flexibility for viewing isolated regions of the data. The graphics source code was designed for LMS and is also written in FORTRAN. This choice was made instead of a "standard" graphics package to provide portability of LMS, to minimize additional core requirements, and to provide graphic capability during execution of an LMS function. This provides direct interactive contact with the results as segmental LMS functions are performed. A special feature of interest in LMS is the inclusion of conversational "help" text, which guides the user through the data entry requirements.

• LMS EXEC routines

Under VM/CMS, an EXEC routine can execute other EXEC routines in a hierarchial fashion. Figure A1 shows a flow chart for the major EXEC routines in LMS. The following is a brief description of some of these routines:

1. MONTY —

Initiates simulation of electron trajectories via Monte Carlo methods to create a spatial distribution in the form of a two-dimensional histogram of energy deposition due to a δ -function source. Random numbers determine the electron-scattering angles

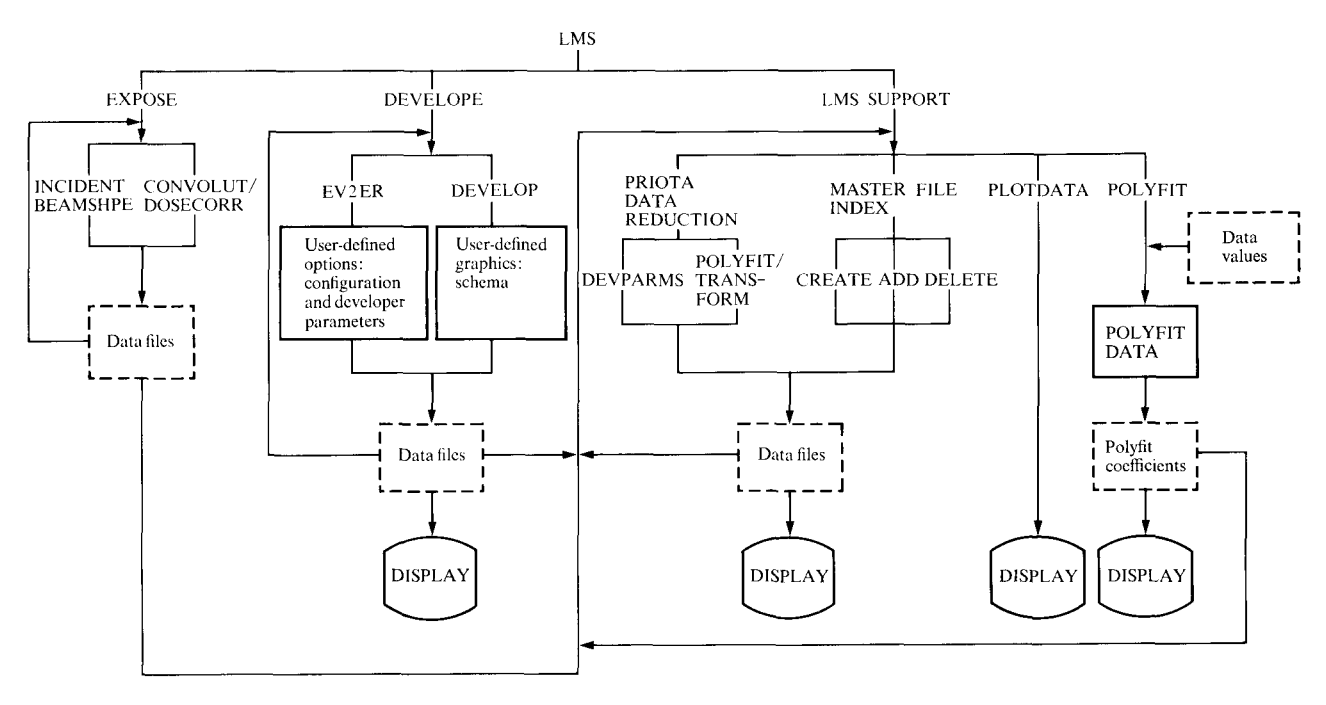


Figure A1 Flow chart of the Lithography Modeling System (LMS).

and, while the electron is in a multicomponent environment, the particular specie of atom associated with each collision. The initial seed, generally required for random number generation, is obtained from the system clock.

- 2. BEAMSHPE Creates the envelope curve under which the δ -function latent image from MONTY will be calculated. The incident beam shape is defined by Eq. (1) or by a Gaussian. The standard FORTRAN function erf is used with the distance between each lateral δ-function point equivalent to the cell dimensions assigned during the execution of MONTY.
- 3. CONVOLUT This algorithm convolutes a Monte Carlo distribution under the envelope shape created by BEAMSHPE. In the case of dissimilar electron flux of neighbors in the incident beam shape, convolution is carried out by superposition. Otherwise, convolution is achieved with the aid of
- 4. DEVELOPE This EXEC executes either or both of two source routines: 1) EV2ER, 2) DEVELOP. EV2ER uses the ab-

the principle of reciprocity [2].

- sorbed energy density function defined by the user to transform the absorbed energy density latent image created by CONVOLUT to solubility. DEVELOP removes the regions within which the elapsed time of simulated development is equal to or exceeds the time of development of each of the regions (cells). Both the original and supplementary arrays are used to contain pointer values relating positional indices for the tracking of those particular cells in the liquid/solid interface.
- 5. DEVPARMS —
- This EXEC governs the sequential execution of several EXEC routines that in turn execute the source algorithms that result in the values of the parameters in Eq. (3). The required data base includes values of depth remaining vs. the elapsed time of development of large regions. Unexposed and exposed regions at several doses must be available. The sequential stream normally follows this sequence: i) estimate A and a, ii) estimate B and the energy exponent n, iii) estimate the energy-dependent surface rate ε .

435

Figure A2 Sample I/O of graphics terminal sessions with LMS: BEAMSHPE EXEC—definition of incident beam profile; CONVOLUT EXEC—convolution of a Monte Carlo spectrum with beam profile from the preceding routine; DEVELOPE EXEC—time evolution of the developed profile after formation of latent image from the preceding routine. Terminal inputs by the user are designated by asterisks.

```
CMS

* convolut exec

WE WILL CONVOLUT A MONTE CARLO FILE UNDER AN INCIDENT BEAM SHAPE ENTER MONTY CARLO DISTRIBUTION TO BE USED, 'XITT', OR, 'HELP'
FILEHAME FILETYPE

* slaublp8 kv25ke20

YOU ARE ALLOWED A LATERAL SPAN BETWEEN
-11.52 AND 11.57 MICROMS
ENTER ... WITH STON INCLUDED, AND,
THE CENTER OF THE PRINCIPLE LINE AS REFERENCE
THE LEFTHOST AND RIGHTMOST LATERAL DISTANCE(IN MICRONS)
?
*-2.5 2.5

SISUB1P8 KV25Ke20 LWDTH* 2.0 EGWT*0.25 OFFSET(MIC)* 0.0

MOTE!!!!! DOSE RATIOS NOT YET ON TITLE FILE, THEREFOR,
THIS FACT WILL NOT BE CARRIED THROUGH FOR GRAPHICS AND
DEVELOP ROUTINES.

TO PLOT THE RESULTS EXECUTE EITHER:
(1) PLOTDATA CONVOLUT BEATHSHEE
```

```
CMS
* develope exec
   ***** PRESS RETURN FOR PROGRAMED DEFAULTS *****
   36 ROWS 101COLUMNS ON FILE
ENTER DZ SIZE IN MICRONS..AN EOF WILL PUT DZ*.50000E-01MICRONS
NOTE!!!..THE MINIMUM IS.16667E-01MICRONS
          OF .25000E-01AND A DX OF.25000E-01IS BEING USED
E ARE 72 LAYERS AND 202 COLUMNS
R ONE OF THE FOLLOWING OPTIONS:
          HELP
XITT
TAB KEY FOR THE TYPE ON FILE
           FUNC, THE USER DEFINED FUNTION....SOLB...
EOF(RETURN) TO USE PREVIOUSLY CALC. SOLUBILITIES
TEST
   ENTER THE VALUES BEGINNING WITH DP..
DEFAULTFOR DP IS THE FULL DEPTH
DEFAULT FOR RECORD IS VALUES ON FILE
   NOTE! RIGHT ADJUST ALL E FORMAT INPUT. * IS LAST COL
                                    RZERO
   DPT1 STDF DP ALPHA
                                                         ENGEXP
                                                                         ENGCOEF
                                                                                      ITIME(S)
                                                                                           .0
                                                                                                        20.0
                                         .0
50.0
                                                                         2.5e-18
   ENTER THE ENERGY DEPENDENT SURFACE RATE VALUES OR PRESS RETURN FOR THE FOLLOWING DEFAULT VALUES....
    ...... V1-0.0 V2-0.0
* 0.5 2.0e-30 1.5
```

ALL PARAMETER INFORMATION SEEMS COMPLETE

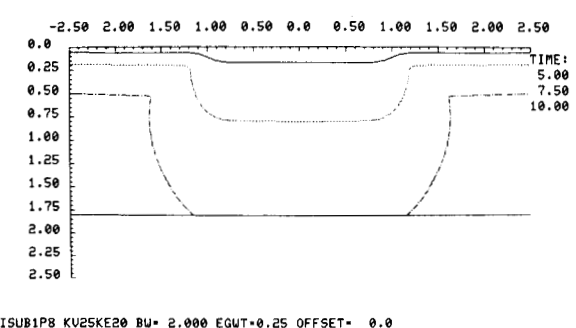
DO YOU WISH TO CONTINUE INTO DEVELOP? ...YES OR NO

```
CHECUTION MOINS...

ENTER OPTION(A4) AND VALUE(DECIMAL)
THE FOLLOWING OPTIONS EXIST
TIME: 1 ADJACENT VALUE(MINUTES)
DPTH: 1 ADJACENT VALUE (MINUTES)
THE NO VALUES REQD. CHOOSES OF THE THE CHARACTER ENTER THE CHARACTER THE CHARACTER THE CHARACTER ENTER THE CHARACTER THE CH
```

Figure A3 Final graphics display of the developed profiles at times of 5, 7.5, and 10 minutes. The vertical axis corresponds to the developed resist thickness (μ m); the horizontal line indicates a total resist thickness of 1.8 μ m. The horizontal axis corresponds to the distance from the center of the developed line (μ m).

DPT1 STDF DP ALPHA RZERO ENGEXP ENGCOEF ITIME(S) DOSE 1.88 - 1.500 50.00 1.050 .2500D-17.0 20.00 50.00 SURFACE VALUES (VI,VZ,V3) ARE: .5000D-00 .20000D-29 .15000D+01



SISUB1P8 KV25KE20 BU- 2.000 EGWT-0.25 OFFSET- 0.0 GRAPHIC CELL SIZE - 256.ANGS10237 CELLS 6 CPU SEC OPTIONS : TIME 5.0,TIME 7.5,TIME 10.0,

The developer algorithm has the following user-defined options available:

- TIME VALU defines the time of development in the profile simulation;
- DPTH VALU defines the depth of development, i.e., the profile which just reaches that depth;
- OPEN VALU defines the width of development,
 i.e., the open dimension of the profile at a particular depth;
- XHAR defines the point on a desired profile using the cross-hair mode of the graphics terminal as a pointer.

Figures A2 and A3 present sample I/O graphics terminal outputs for LMS programs.

Acknowledgments

The authors wish to thank all those who have supported this project, especially H. Ezrol, J. Raniseski, J. Lounsbury, and L. Bushnell of the IBM Data Systems Division (DSD) laboratory in East Fishkill, New York, and A. Sporer, L. Rosier, and C. Ting of the IBM Research Division laboratory in San Jose, California. They have provided much encouragement and the necessary environment, without which it would not have been possible to develop LMS. Technical interaction with N. Viswanathan (DSD, East Fishkill) was very helpful and F. Jones (IBM Research Division, Yorktown Heights, New York) assisted in the analysis of solubility rate data leading to the form of Eq. (3). We also thank Prof. A. Neureuther of the University of California at Berkeley for many valuable and stimulating discussions as a consultant in computer simulation of lithographic processes.

References and note

- A. N. Broers and T. H. P. Chang, "High Resolution Lithography for Microcircuits," Microcircuit Engineering, H. Ahmed and W. C. Nixon, Eds., Cambridge University Press, Cambridge, England, to be published. Also available as Research Report RC-7403, IBM Thomas J. Watson Research Center, Yorktown Heights, NY, 1978.
- T. H. P. Chang, "Proximity Effect in Electron Beam Lithography," J. Vac. Sci. Technol. 12, 1271 (1975).
- 3. D. F. Kyser and N. S. Viswanathan, "Monte Carlo Simulation of Spatially Distributed Beams in Electron Beam Lithography," J. Vac. Sci. Technol. 12, 1305 (1975).
- 4. D. F. Kyser and K. Murata, "Monte Carlo Simulation of Electron Beam Scattering and Energy Loss in Thin Films," Proceedings of the Sixth International Conference on Electron and Ion Beam Science and Technology, San Francisco, CA, 1974; R. Bakish, Ed., The Electrochemical Society, Princeton, NJ, p. 205.
- M. Parikh and D. F. Kyser, "Energy Deposition Functions in Electron Resist Films on Substrates," J. Appl. Phys. 50, 1104 (1979).
- 6. T. H. P. Chang, A. D. Wilson, A. J. Speth, and C. H. Ting, "Vector Scan I: An Automated Electron Beam System for High Resolution Lithography," Proceedings of the Seventh International Conference on Electron and Ion Beam Science and Technology, Washington, DC, 1976; R. Bakish, Ed., The Electrochemical Society, Princeton, NJ, p. 392.
- H. C. Pfeiffer, "New Imaging and Deflection Concept for Probe-forming Microfabrication Systems," J. Vac. Sci. Technol. 12, 1170 (1975).
- F. H. Dill, A. R. Neureuther, J. A. Tuttle, and E. J. Walker, "Modeling Projection Printing of Positive Photoresists," *IEEE Trans. Electron Devices* ED-22, 456 (1975).

- J. B. Lounsbury and M. A. Narasimham, "Dissolution Rate Analysis of Some Positive Photoresist Systems," Abstracts of Papers, 174th ACS National Meeting, Chicago, IL, 1977 (Organic Coatings and Plastics Chemistry Division), Port City Press, Inc., Baltimore, MD, 1977.
- Jane M. Shaw and Michael Hatzakis, "Performance Characteristics of Diazo-type Photoresists Under E-Beam and Optical Exposure," *IEEE Trans. Electron Devices* ED-25, 425 (1978).
- M. Hatzakis, C. H. Ting, and N. S. Viswanathan, "Fundamental Aspects of Electron Beam Exposure of Polymeric Resist Systems," Ref. 4, loc. cit., p. 542.
- J. S. Greeneich, "Developer Characteristics of PMMA Electron Resist," J. Electrochem. Soc. 122, 970 (1975).
- A. R. Neureuther, D. F. Kyser, and C. H. Ting, "Electron Beam Resist Edge Profile Simulation," *IEEE Trans. Elec*tron Devices ED-26, 686 (1979).
- 14. *AZ is a registered trademark of the Azoplate Division of American Hoechst Corp., Somerville, NJ 08876. The material was supplied by Shipley Co., Newton, MA.
- M. Hatzakis, "Recent Developments in Electron-Resist Evaluation Techniques," J. Vac. Sci. Technol. 12, 1276 (1975).
- M. Parikh, "SPECTRE—A Self Consistent Proximity Effect Correction Technique for Resist Exposure," J. Vac. Sci. Technol. 15, 931 (1978).
- W. D. Grobman, H. E. Luhn, T. P. Donohue, A. J. Speth, A. D. Wilson, M. Hatzakis, and T. H. P. Chang, "1 μm MOSFET-VLSI Technology: Part VI—Electron-Beam Lithography," *IEEE Trans. Electron Devices* ED-26, 360 (1979) and *IEEE J. Solid-State Circuits* SC-14, 282 (1979) (proceedings published jointly).
- 18. D. F. Kyser, D. E. Schrieber, C. H. Ting, and R. Pyle, "Proximity Function Approximations for Electron Beam Lithography from Resist Profile Simulation," Proceedings of the Ninth International Conference on Electron and Ion Beam Science and Technology, St. Louis, MO, 1980; The Electrochemical Society, Princeton, NJ, to be published.
- Mihir Parikh, "Proximity Effects in Electron Lithography: Magnitude and Correction Techniques," IBM J. Res. Develop. 24, 438 (1980, this issue).

Received May 25, 1979; revised April 21, 1980

D. F. Kyser is located at the IBM Research Division laboratory, 5600 Cottle Road, San Jose, California 95193; R. Pyle is located at the IBM Data Systems Division laboratory, East Fishkill (Hopewell Junction), New York 12533.